JCI The Journal of Clinical Investigation

# Male infertility, impaired spermatogenesis, and azoospermia in mice deficient for the pseudophosphatase Sbf1

Ron Firestein, … , Marco Conti, Michael L. Cleary

*J Clin Invest.* 2002;109(9):1165-1172. https://doi.org/10.1172/JCI12589.

Article Genetics

Pseudophosphatases display extensive sequence similarities to phosphatases but harbor amino acid alterations in their active-site consensus motifs that render them catalytically inactive. A potential role in substrate trapping or docking has been proposed, but the specific requirements for pseudophosphatases during development and differentiation are unknown. We demonstrate here that Sbf1, a pseudophosphatase of the myotubularin family, is expressed at high levels in seminiferous tubules of the testis, specifically in Sertoli's cells, spermatogonia, and pachytene spermatocytes, but not in postmeiotic round spermatids. Mice that are nullizygous for Sbf1 exhibit male infertility characterized by azoospermia. The onset of the spermatogenic defect occurs in the first wave of spermatogenesis at 17 days after birth during the synchronized progression of pachytene spermatocytes to haploid spermatids. Vacuolation of the Sertoli's cells is the earliest observed phenotype and is followed by reduced formation of spermatids and eventual depletion of the germ cell compartment in older mice. The nullizygous phenotype in conjunction with high-level expression of Sbf1 in premeiotic germ cells and Sertoli's cells is consistent with a crucial role for Sbf1 in transition from diploid to haploid spermatocytes. These studies demonstrate an essential role for a pseudophosphatase and implicate signaling pathways regulated by myotubularin family proteins in spermatogenesis and germ cell differentiation.



# Male infertility, impaired spermatogenesis, and azoospermia in mice deficient for the pseudophosphatase Sbf1

Ron Firestein,[1] Peter L. Nagy,[1] Megan Daly,[1] Phil Huie,[1] Marco Conti,[2] and Michael L. Cleary[1]

[1]Department of Pathology, and
[2]Department of Obstetrics and Gynecology, Stanford University School of Medicine, Stanford, California, USA

Address correspondence to: Michael L. Cleary, Department of Pathology, Stanford University School of Medicine, 300 Pasteur Drive, Stanford, California 94305, USA.
Phone: (650) 723-5471; Fax: (650) 498-6222; E-mail: mcleary@stanford.edu.

Received for publication April 23, 2001, and accepted in revised form March 25, 2002.

**Pseudophosphatases display extensive sequence similarities to phosphatases but harbor amino acid alterations in their active-site consensus motifs that render them catalytically inactive. A potential role in substrate trapping or docking has been proposed, but the specific requirements for pseudophosphatases during development and differentiation are unknown. We demonstrate here that Sbf1, a pseudophosphatase of the myotubularin family, is expressed at high levels in seminiferous tubules of the testis, specifically in Sertoli's cells, spermatogonia, and pachytene spermatocytes, but not in postmeiotic round spermatids. Mice that are nullizygous for Sbf1 exhibit male infertility characterized by azoospermia. The onset of the spermatogenic defect occurs in the first wave of spermatogenesis at 17 days after birth during the synchronized progression of pachytene spermatocytes to haploid spermatids. Vacuolation of the Sertoli's cells is the earliest observed phenotype and is followed by reduced formation of spermatids and eventual depletion of the germ cell compartment in older mice. The nullizygous phenotype in conjunction with high-level expression of Sbf1 in premeiotic germ cells and Sertoli's cells is consistent with a crucial role for Sbf1 in transition from diploid to haploid spermatocytes. These studies demonstrate an essential role for a pseudophosphatase and implicate signaling pathways regulated by myotubularin family proteins in spermatogenesis and germ cell differentiation.**

*J. Clin. Invest.* **109**:1165–1172 (2002). DOI:10.1172/JCI200212589.

## Introduction

Protein tyrosine and dual-specificity phosphatases participate in diverse physiological processes. In conjunction with kinases, they regulate the phosphorylation states of proteins and lipids in various subcellular compartments, thereby impinging on many aspects of cellular function (1). Recent studies have identified an additional component of this catalytic hierarchy, the so-called pseudophosphatases (2, 3), which display extensive sequence similarities to phosphatases, but harbor inactivating mutations in their active-site consensus motifs that render them catalytically inactive. Several proteins with pseudophosphatase features have been identified (2), most of which are conserved throughout metazoan evolution. Several are similar to myotubularin, a phosphatase that was originally discovered by virtue of its mutation in a subset of patients with X-linked myotubular myopathy (4, 5). Myotubularin belongs to a growing subgroup of phosphatases that dephosphorylate lipid substrates (6) and is one of several lipid phosphatases whose mutations are associated with heritable disorders of aberrant growth or differentiation (6–8).

Sbf1 (SET-binding factor 1 or MTMr5) is the most extensively characterized of the myotubularin-related pseudophosphatases. It is a 220-kDa cytoplasmic protein that was initially identified based on its in vitro interaction with MLL, a proto-oncogenic protein involved by chromosomal translocations in mixed lineage leukemias (5, 9). Sbf1 contains several domains (e.g., pleckstrin and Rab3 GEF homology motifs) that are conserved in signaling proteins, and in vitro studies suggest a role for Sbf1 in cellular growth control (5, 9–11). The ability of Sbf1 to modulate cellular growth, however, is abrogated by restoring catalytic activity to its phosphatase homology domain. Based on these and other observations, it has been hypothesized that pseudophosphatases may contribute to cellular homeostasis by opposing the actions of phosphatases (3), perhaps as naturally occurring substrate-trapping mutants analogous to experimentally inactivated phosphatases, which bind phosphorylated substrates and prevent their dephosphorylation (12). Alternatively, the inactivated catalytic pockets of pseudophosphatases may serve as docking motifs for phosphorylated substrates analogous to the roles of SH2 and PTB motifs (2). Regardless of their biochemical mechanisms of action, little is known about the developmental roles of pseudophosphatases. Here, we demonstrate that the presence of Sbf1 is required for male reproductive function. Our studies

further reveal that Sbf1 is specifically required for spermatogenesis through contributions to male germ cell differentiation and survival.

## Methods

*Targeted disruption of the Sbf1 gene*. Appropriate *Sbf1* genomic DNA fragments (129SV) were cloned into the pNT targeting vector such that the *Pgk-Neo* cassette replaced exons 21–28 of the *Sbf1* gene. The targeting construct was linearized and transfected into embryonic stem (ES) cells using standard conditions (Genome Systems Inc., St. Louis, Missouri, USA). Six out of 195 ES cell clones that survived selection in G418 had undergone homologous recombination as determined by Southern blotting with DNA probes external to the targeting construct (probe A: 600-bp NotI-XhoI; or probe B: 1.1-kb XhoI). Euploid, targeted ES cell clones were introduced into C57BL/6 blastocysts by microinjection. Male offspring that displayed high-percentage coat-color chimerism were crossed with C57BL/6 females resulting in germline transmission of the disrupted *Sbf1* allele. Nullizygous males from backcrossed generations generally exhibited reduced postnatal viability of undetermined cause. The testicular phenotype was predominantly characterized in the $F_1$ generation and shown to be identical to that in the occasional backcrossed males that survived.

*Genotyping and blotting analyses*. Genotyping was performed either by PCR (primers and conditions available upon request) or Southern blot analysis with probes A and B. Total RNA (10 μg/lane) isolated from tissues of 8-week-old mice was examined by Northern blot analysis using a mouse *Sbf1* cDNA probe (bp 1,033–1,870). Total RNA (10 μg/lane) pooled from four to six staged testes was used for Northern blot analysis using mouse cDNA probes for calspermin (bp 274–854), DMC1 (bp 814–1,300), Hsp25 (bp 50–665), and β-actin (supplied by Ambion Inc., Austin, Texas, USA). A human *Sbf1* cDNA probe (bp 1,800–5,700) was used for Northern blot analysis of commercially prepared RNA from human tissues (CLONTECH Laboratories Inc., Palo Alto, California, USA). For Western blot analyses, tissues or cells were washed in PBS and immediately homogenized in 1× SDS lysis buffer (2% SDS, 100 mM Tris, pH 6.8, 10% glycerol) followed by centrifugation at 12,000 *g* at 4°C for 5 minutes. Proteins in the supernatant (50 μg) were resolved by SDS-PAGE, transferred to membranes, and incubated with either an anti-Sbf1 mAb (9) or a mouse antiserum raised against a maltose-binding protein (MBP) fusion protein containing the N-terminal 200 amino acids of Sbf1.

*Fertility, mating behavior, and endocrine assays*. Fertility was evaluated by scoring for pregnancies following exposure of male mice to wild-type C57BL/6 females for at least 3 months' duration. Mating behavior was evaluated by observation of males after introduction of a female into the cage. At the end of the mating regimen, reproductive organs were harvested for determination of weights and sperm counts. Spermatozoal quality was determined by light microscopy, and quantity was measured by hematocytometry. Serum levels of follicle-stimulating hormone (FSH), leutenizing hormone (LH), and testosterone (serum T) were determined by radioimmunoassay (AniLytics Inc., Gaithersburg, Maryland, USA) on age-matched mice at 3 months of age.

*Pathological examinations*. Reproductive organs were removed from prepubertal, pubertal, or adult male mice for gross and histological analysis. Tissues were immediately fixed in buffered formalin or Bouin's fixative, embedded in paraffin, sectioned (4 μm), and then stained with hematoxylin and eosin using standard procedures. For electron microscopy, testes were fixed with 2.5% glutaraldehyde/2% paraformaldehyde in sodium cacodylate buffer overnight at 4°C. The tissue was then washed in several changes of sodium cacodylate buffer and incubated in 2% osmium tetroxide overnight at 4°C. The samples were then washed with distilled water, dehydrated in a series of ethanols, washed with propylene oxide, and embedded in LX-112 (Ladd Research Industries, Williston, Vermont, USA). Thin sections were stained with uranyl acetate and lead citrate and examined by electron microscopy using a Hitachi EM300 (Hitachi Instruments, Naperville, Illinois, USA).

*Immunohistochemistry and in situ hybridization*. Immunohistochemical detection of Sbf1 was performed on formalin-fixed, paraffin-embedded tissues following antigen retrieval consisting of microwave treatment for 15 minutes in a 0.5 M Tris, pH 10, solution. The primary Ab consisted of a mouse mAb (mAb 68) specific for Sbf1 (9). Immune complexes were detected using biotinylated anti-mouse serum and avidin horseradish-peroxidase complexes. In situ hybridization was performed on adult wild-type testis as described previously (13). The probes consisted of sense and antisense *Sbf1* transcripts generated by T3 and T7 polymerases, respectively, using a linearized pBluescriptII vector containing 500 bp of the mouse *Sbf1* cDNA.

*Apoptosis assays*. Apoptosis was evaluated using a TUNEL assay for in situ visualization of DNA fragmentation. TUNEL assays were performed using commercially prepared reagents (Apoptag; Intergen Co., Purchase, New York, USA) on sections of testis that had been fixed in 4% paraformaldehyde for 20 hours and embedded in paraffin. For each testis, TUNEL-labeled (apoptotic) nuclei in 30 seminiferous tubules were counted and averaged as described previously (14).

## Results

*Differential expression of Sbf1 in the seminiferous tubules*. Northern blot analysis of RNA isolated from adult mouse tissues demonstrated expression of *Sbf1* at high levels in the testis and at lower levels in the brain and colon. Analysis of human tissues similarly revealed highest levels of *Sbf1* expression in the testis (Figure 1a). Western blot analysis of proteins isolated

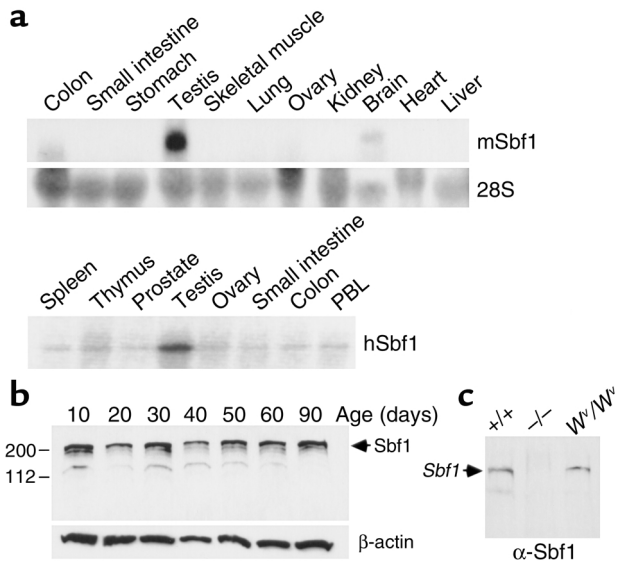


**Figure 1**
Tissue-specific expression of Sbf1. (**a**) Northern blot analysis of total RNA prepared from human tissues or adult mice. The hybridization probe consisted of an *Sbf1* cDNA (upper panel). Abundance of 28S rRNA is shown for the mouse blot for comparison. (**b**) Western blot analysis of protein extracts from testes at different stages of spermatogenic development. Migration of Sbf1 (upper panel) and β-actin (loading control, lower panel) is indicated. Faint bands in some lanes at 150 kDa represent apparent Sbf1 degradation products. (**c**) Anti-Sbf1 Western blot analysis of protein extracts from wild-type, *Sbf1*$^{-/-}$, and *W*$^{v}$/*W*$^{v}$ adult mice.

from testes at postnatal days 20–90 showed that expression of Sbf1 was relatively constant throughout progression of spermatogenesis, which is highly synchronized during this time period (Figure 1b). Notably, Sbf1 was also detected in prepubertal testis (day 10), suggesting that it was expressed by either spermatogonia, preleptotene spermatocytes, or Sertoli's cells. These observations raised the possibility of a role for Sbf1 in germ cell function during spermatogenesis, the ordered process of germ cell mitosis, meiosis, and differentiation into sperm (14).

To investigate the role of Sbf1 in spermatogenesis, its expression was evaluated by in situ analyses of testes from adult and juvenile mice. In situ hybridization demonstrated that *Sbf1* mRNA was most prominently expressed within seminiferous tubules of adult testis at the basal regions that contain spermatogonia, spermatocytes, and Sertoli's cells (Figure 2a). In agreement with the in situ hybridization data, immunohistochemical analysis of Sbf1 protein distribution in testes at different days of development revealed that it was prominently expressed in Sertoli's cells, spermatogonia, and pachytene spermatocytes, but was notably absent in postmeiotic round spermatids (Figure 2, c and e). Its predominant cytoplasmic localization was consistent with more extensive studies of its subcellular distribution (5). Western blot and immunohistochemical analysis of testes from *W*$^{v}$/*W*$^{v}$ mice, which lack germ cells but contain Sertoli's cells, confirmed that the latter express cytoplasmic Sbf1 (Figure 1c and Figure 2g). The observed expression profiles of Sbf1 in the seminiferous tubules of pubertal mice suggested a function in the early stages of germ cell differentiation.

*Male Sbf1*$^{-/-}$ *mice are infertile with azoospermia*. To establish the role of *Sbf1* in normal mouse development and physiology, a loss-of-function mutation was introduced into the gene by homologous recombination. The targeting vector was engineered to inactivate *Sbf1* by replacing exons 21–28 with a *Pgk-Neo* cassette (Figure 3a) to prematurely terminate the recombined allele. The expected wild-type and mutated *Sbf1* alleles were observed by Southern blot analyses of DNA extracted

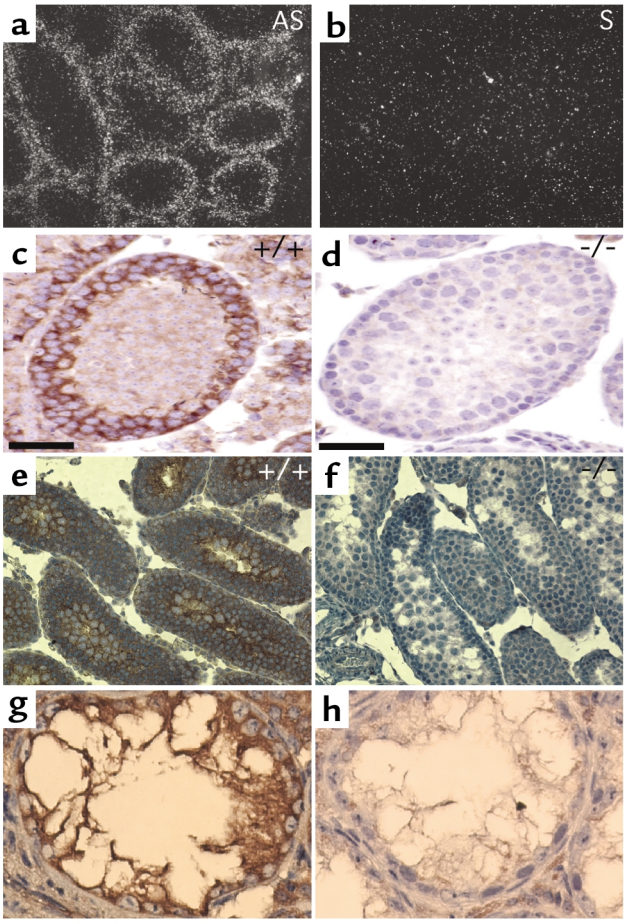


**Figure 2**
Sbf1 expression in testis. (**a** and **b**) In situ hybridization of wild-type adult mouse testis demonstrates specific expression of *Sbf1* mRNA transcripts in the basilar portions of the seminiferous tubules. Sections were hybridized with antisense (AS) and sense (S) *Sbf1*-specific riboprobes as indicated (×200). (**c** and **d**) Immunohistochemical analysis demonstrates Sbf1 protein expression in cells at the periphery of seminiferous tubules in wild-type (+/+) but not *Sbf1*$^{-/-}$ (–/–) mice at 4 weeks of age (×400). Scale bars, 25 μm. (**e** and **f**) Sbf1 protein is detected by immunohistochemistry in cells of the immature testis (day 16) in wild-type (+/+) but not *Sbf1*$^{-/-}$ (–/–) mice (×200). (**g** and **h**) Immunohistochemical detection of Sbf1 protein in seminiferous tubules of adult *W*$^{v}$/*W*$^{v}$ mice shows Sbf1 expression in Sertoli's cells. Control (**h**) represents secondary Ab alone.

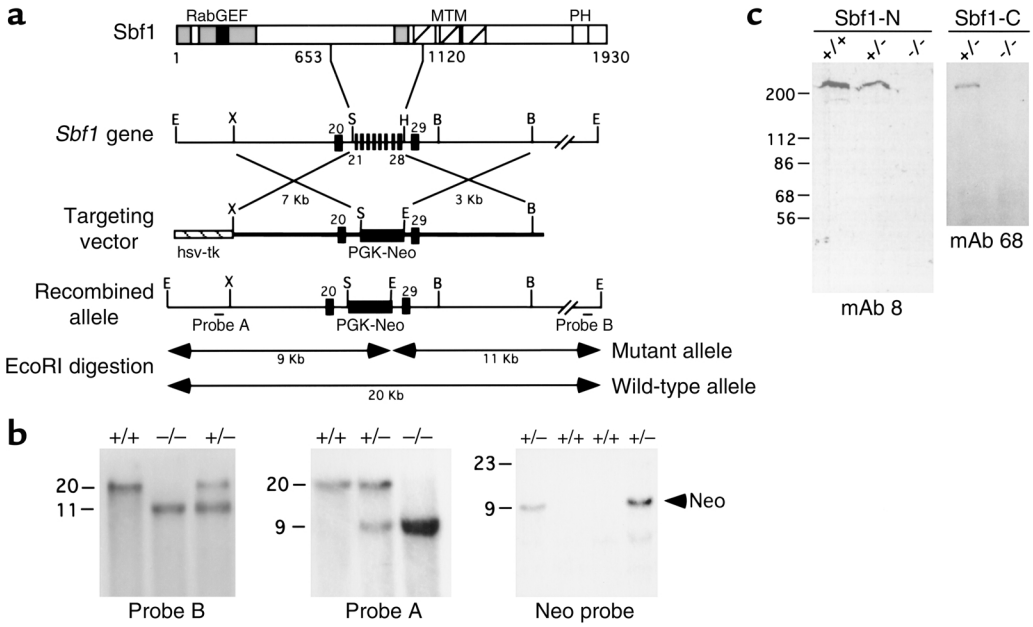


**Figure 3**
Targeted disruption of the *Sbf1* gene. (**a**) Schematic depiction of the Sbf1 protein, gene, targeting construct, and recombined allele. Conserved motifs present in Sbf1 include an N-terminal Rab GEF homology domain, internal MTM homology motifs, and a C-terminal PH domain. Following homologous recombination, a *Pgk-Neo* cassette replaces *Sbf1* exons 21–28, which encode amino acids 653–1120 of the Sbf1 protein as indicated. Locations are shown for external probes A and B used for genotype analyses. Restriction enzyme sites: E, EcoRI; X, XhoI; S, SacI; H, HindIII; B, BamH1. (**b**) Southern blot analysis of genomic DNA isolated from wild-type (+/+), $Sbf1^{+/-}$ (+/–), and $Sbf1^{-/-}$ (–/–) mice. Probes are indicated below the respective panels. (**c**) Western blot analysis of brain extracts of wild-type (+/+), $Sbf1^{+/-}$ (+/–), or $Sbf1^{-/-}$ (–/–) mice. Primary Ab's (indicated below panels) consisted of mAb's specific for the N-terminal (mAb 8) or C-terminal (mAb 68) portions of Sbf1. Faint bands in some lanes at 150 kDa represent apparent Sbf1 degradation products.

from targeted ES cell lines (not shown) and mouse tissues (Figure 3b). Western blot analysis showed that $Sbf1^{-/-}$ mice expressed neither full-length nor truncated portions of Sbf1 (Figure 3c). Immunohistochemical analysis of seminiferous tubules of $Sbf1^{-/-}$ juvenile and prepubertal mice confirmed the absence of Sbf1 in spermatogonia, pachytene spermatocytes, and Sertoli's cells (Figure 2, d and f).

Intercrossing of F1 $Sbf1^{+/-}$ mice showed that $Sbf1^{-/-}$ progeny were born at the expected Mendelian ratios, were viable, and reached adulthood. Nullizygous males from backcrossed generations, however, exhibited reduced postnatal viability (wild-type, 17; heterozygote, 44; homozygous null, 7; 0 males, at 3 weeks). $Sbf1^{-/-}$ males were infertile and incapable of siring offspring, in contrast to the normal fertility and fecundity of $Sbf1^{+/-}$ males and $Sbf1^{-/-}$ females (Table 1). Evaluation of the mating behavior of $Sbf1^{-/-}$ males showed that they copulated with females at a rate comparable to wild-type males (data not shown), suggesting that behavioral factors were not the cause of infertility. The external genitalia and testicular descent of $Sbf1^{-/-}$ males appeared normal, but testis sizes and weights were markedly reduced compared with either heterozygous or wild-type males (Table 2, Figure 4, a and b). Furthermore, sperm counts and epididymal histology revealed the lack of sperm within the epididymi of $Sbf1^{-/-}$ mice (Table 2, Figure 4, c and d).

The pituitary hormones FSH and LH (through testosterone secretion) regulate spermatogenesis and prevent the germ cell compartment from undergoing apoptosis. These hormones are first expressed during puberty in the male mouse and are required throughout adulthood to maintain spermatogenesis. Serum levels of FSH, LH, and testosterone at 12 weeks of age were not significantly different in $Sbf1^{-/-}$ compared with wild-type littermates (Table 3), indicating that the testicular defects were not caused by reduced levels of these hormones.

The seminiferous tubules of $Sbf1^{-/-}$ mice were evaluated for perturbations in spermatogenesis. Histological examination of adult testes revealed extensive vacuolation of the tubules accompanied by a decrease in the number of round spermatids, very few elongating spermatids, and no mature sperm in $Sbf1^{-/-}$ mice

**Table 1**
Infertility phenotype of male *Sbf1* mutant mice

| Breeding pair M × F | | Pairs mated (no.) | Litters (no.) | Litter size[A] |
|---|---|---|---|---|
| +/+ | +/+ | 3 | 3 | 9 ± 1 |
| +/– | +/+ | 5 | 5 | 8 ± 1 |
| –/– | +/+ | 4 | 0 | NA |
| +/+ | –/– | 5 | 5 | 6 ± 2 |

[A]Values represent mean ± SD.

**Table 2**
Sterility of *Sbf1*$^{-/-}$ male mice

| Sbf1 genotype | Testis weight (mg) | Epididymis/vas deference weight (mg) | Sperm count/ epididymis (×10$^6$) |
|---|---|---|---|
| +/+ | 105 ± 15 | 50 ± 5 | 18 ± 2 |
| +/– | 85 ± 12 | 45 ± 7 | 20 ± 4 |
| –/– | 35 ± 4 | 35 ± 5 | 0 |

Reproductive organs were removed from mice at 20 weeks of age. All values represent the mean ± SD.

(Figure 4, k and l). Germ cell differentiation was disorganized, lacking the characteristic basal-to-luminal maturation observed in normal seminiferous tubules. By 52 weeks of age, few germ cells remained within *Sbf1*$^{-/-}$ tubules, although Sertoli's cells persisted (Figure 4, m and n) and marked interstitial hyperplasia of Leydig's cells was observed. These data indicated that the primary phenotype of adult *Sbf1*$^{-/-}$ mice was a progressive spermatogenic failure.

*Sbf1*$^{-/-}$ *mice display defects in the first wave of spermatogenesis*. The severe pathological findings in testes of adult *Sbf1*$^{-/-}$ mice prompted examination at earlier times of postnatal development. Spermatogenesis begins neonatally in the mouse, and the first wave of germ cell differentiation is synchronized such that all tubules are at the same stage of spermatogenesis (15). In sexually immature mice at 10 days of age, a time at which germ cell meiosis has begun, seminiferous tubules of *Sbf1*$^{-/-}$ mice were comparable in both size and morphology to their wild-type littermates (Figure 4, e and f). Examination of testes at days 14 and 16 revealed no histopathology (data not shown). Histologic aberrations were first detected at day 17 in *Sbf1*$^{-/-}$ testes (Figure 4, g and h) and consisted of vacuoles that appeared to be associated with Sertoli's cells as seen by light microscopic analysis (Figure 5a). Electron microscopy revealed that the vacuoles were completely within the cytoplasm of Sertoli's cells in multiple electron microscope montages examined (Figure 5b).

By 20 days of age, when germ cells in testes of wild-type mice had completed the second meiotic division and progressed to the haploid round spermatid stage, the seminiferous tubules of *Sbf1*$^{-/-}$ mice showed reduced numbers of round spermatids and increased vacuolization (Figure 4, i and j). Tubular pathology progressively worsened in subsequent days with further decrease in spermatids at all stages of differentiation and the appearance of apoptotic bodies. These observations localized the onset of the spermatogenetic defect to the stage when pachytene spermatocytes progress to round spermatids.

To more clearly delineate when the *Sbf1* nullizygous defect occurs, we examined molecular markers expressed at specific stages of germ cell development. These included genes expressed in leptotene to zygotene spermatocytes (DMC1), leptotene to pachytene spermatocytes (Hsp25), and spermatids (calspermin) (16–18). Northern blot analysis of DMC1

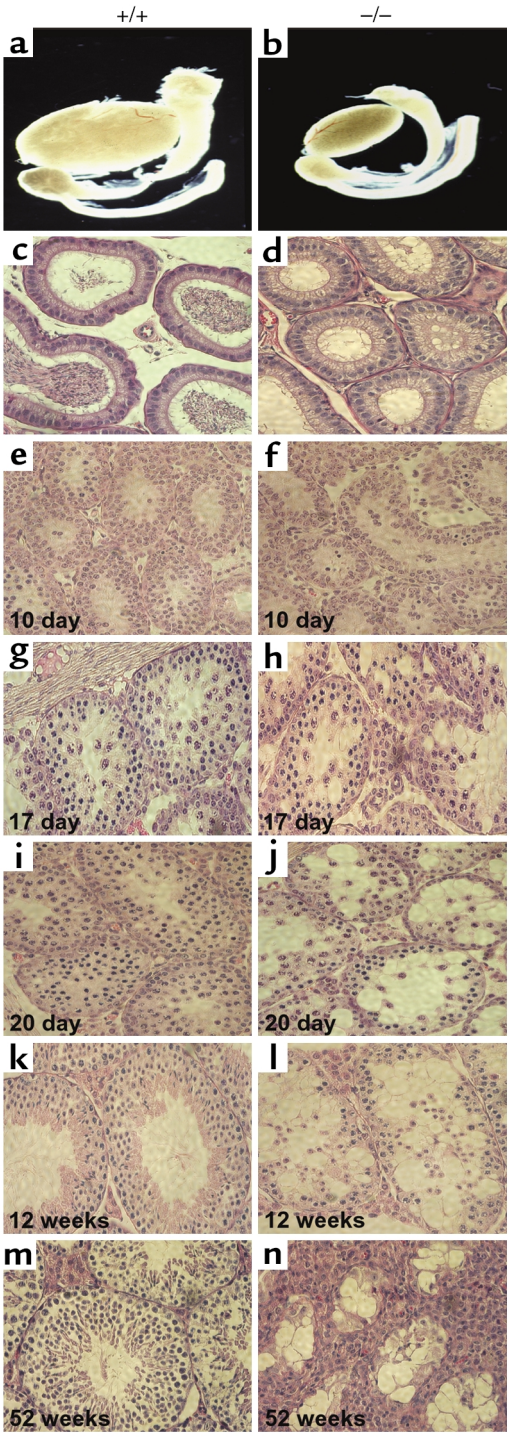


**Figure 4**
Failure of spermatogenesis in *Sbf1*$^{-/-}$ mice. Comparative anatomy and histology are shown for wild-type (+/+) and Sbf1$^{-/-}$ (–/–) testes. (**a** and **b**) Male reproductive organs are shown for mice at 20 weeks of age. *Sbf1*$^{-/-}$ testis, but not epididymis, is considerably smaller compared with wild-type (×2). (**c** and **d**) Sections of epididymis from 20-week-old mice were stained with hematoxylin and eosin (×200). Note absence of spermatozoa in *Sbf1*$^{-/-}$ epididymis. (**e**–**n**) Sections of wild-type and *Sbf1*$^{-/-}$ testes at different stages of spermatogenic development (specific time points indicated in the respective panels) were stained with hematoxylin and eosin (×200). Testes from *Sbf1*$^{-/-}$ mice show extensive vacuolar degeneration that is apparent at day 17 and is followed by complete depletion of germ cells by 52 weeks.

**Table 3**
Serum hormone levels of wild-type and *Sbf1*$^{-/-}$ mice at 12 weeks of age

| Hormone | Wild-type | *Sbf1*$^{-/-}$ |
|---|---|---|
| Testosterone | 3.5 ± 3.4 | 1.1 ± 0.9 |
| FSH | 28.8 ± 11.2 | 34.7 ± 8.0 |
| LH | 0.32 ± 0.31 | 0.32 ± 0.30 |

$P > 0.05$ for all hormones tested.

and Hsp25 transcripts through the first wave of spermatogenesis showed that they were expressed at comparable levels in wild-type and *Sbf1*$^{-/-}$ testes. Conversely, calspermin RNA expression was reduced significantly in testes of *Sbf1*$^{-/-}$ mice (Figure 6). These data are consistent with the histological findings that spermatid production is significantly reduced and indicate that spermatocyte viability in *Sbf1*$^{-/-}$ mice is preserved at least into early adulthood.

The possible role of apoptosis in depletion of the germ cell compartment in *Sbf1*$^{-/-}$ male mice was examined by conducting TUNEL assays on testes at different stages of development. Although significant vacuolation (the earliest morphological abnormality) was first observed in *Sbf1*$^{-/-}$ testes at day 17 (Figure 4, g and h), the number of TUNEL-labeled apoptotic nuclei per tubule remained comparable between *Sbf1*$^{-/-}$ and wild-type mice at this time point. At 4–8 weeks of age, however, there was a dramatic increase in the number of apoptotic nuclei in the seminiferous tubules of *Sbf1*$^{-/-}$ mice. At later time points, the apoptotic index decreased in the *Sbf1*$^{-/-}$ tubules as fewer germ cells remained (Figure 7). Taken together, these observations suggested that in the absence of Sbf1 there was a failure in the differentiation of the prehaploid stages of spermatogenesis with consequent induction of programmed cell death in the germ cell compartment. The presence of vacuolization in the Sertoli's cells prior to the onset of apoptosis suggests that Sertoli's cell dysfunction may be the primary stimulus for the aberrant spermatogenic progression and germ cell apoptosis that ensues.

## Discussion

Specific roles for myotubularin family phosphatases in organogenesis and differentiation were suggested previously by their tissue-restricted expression profiles (4, 15) and organ-specific phenotypes in heritable human diseases (4, 7), but the roles for myotubularin-related pseudophosphatases were undefined. Using a loss-of-function mouse model, our current studies demonstrate an essential role for the myotubularin-related pseudophosphatase Sbf1 in spermatogenesis. Hormonal and copulatory studies showed no changes in *Sbf1*$^{-/-}$ mice, indicating a primary spermatogenetic defect. The onset of the spermatogenetic defect occurs in the first wave of spermatogenesis at 17 days after birth during the synchronized progression of pachytene spermatocytes to haploid spermatids. Early disruption of spermatogenesis was evidenced by Sertoli's cell vacuolization and defective germ cell differentiation and tubular disorganization. This was followed by extensive apoptosis and progressive depletion of germ cells, which were completely absent in the seminiferous tubules at 1 year of age. Late onset depletion of spermatogonia and spermatocytes suggests that these features are secondary effects of the disordered spermatogenetic environment.

The temporal onset of the spermatogenic defect in *Sbf1*$^{-/-}$ mice corresponds to the initiation of the meiotic division of pachytene spermatocytes to haploid spermatids at 17–20 days after birth (19). The nullizygous phenotype in conjunction with high-level expression of Sbf1 in premeiotic germ cells and Sertoli's cells is indicative of either a direct or indirect role for Sbf1 in the transition from spermatogonia to haploid spermatocytes. Our findings that vacuolization of Sertoli's cells precedes germ cell apoptosis suggest that dysfunction of Sertoli's cells may be the primary defect in *Sbf1*$^{-/-}$ mice. Sertoli's cells serve a particularly important role during the meiotic stages of the first spermatogenetic cycle. During this time they mediate formation of a tubular lumen, undergo extensive cytoplasmic differentiation, and stimulate

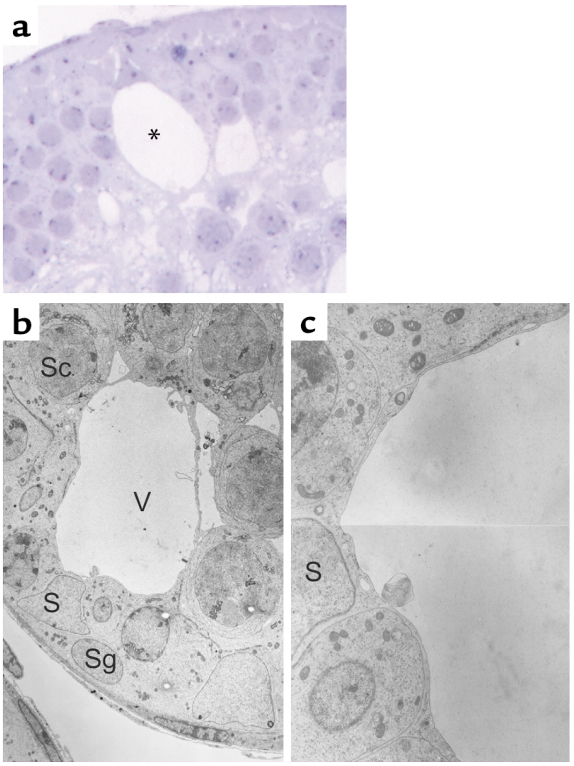


**Figure 5**
Vacuolization of Sertoli's cells at 17 days of age. (**a**) Section of *Sbf1*$^{-/-}$ seminiferous tubules demonstrating a Sertoli's cell with intracytoplasmic vacuole (*) (×400). (**b** and **c**) Electron microscopic analysis of a representative Sertoli's cell and associated vacuole at low (**b**) (×1,500) and high (**c**) (×4,000) magnification. Sertoli's cell (S), spermatogonial cell (Sg), spermatocyte (Sc), and vacuole (V) are indicated.

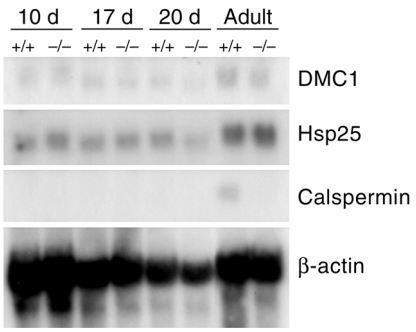


**Figure 6**
Expression analysis of different germ cell markers in *Sbf1*$^{-/-}$ mice. Northern blot of total RNA prepared from mouse testis at different time points of spermatogenic development. Autoradiogram shows transcript levels in *Sbf1*$^{-/-}$ versus wild-type mice probed with $^{32}$P-labeled DMC1, Hsp25, and calspermin cDNAs. The same blot was hybridized with a β-actin probe as a control.

synthetic activity of secretory proteins that direct germ cell differentiation (20). Vacuolization is a common feature of Sertoli's cell dysfunction and injury (21, 22) and is thought to result from swelling of membrane-bound organelles such as the endoplasmic reticulum (23). Since Sbf1 is expressed in Sertoli's cells and a subset of germ cells, it is not clear whether the defect in germ cell differentiation in *Sbf1*$^{-/-}$ mice is cell autonomous or solely the consequence of Sertoli's cell dysfunction. To definitively determine this will require germ cell transplantation experiments (24). Nevertheless, our data demonstrate that Sbf1 is necessary for early events of spermatogenesis that are initiated in the pubertal mouse.

Several proteins with pseudophosphatase features have been identified. The most extensively characterized is STYX, which has been shown recently to be essential for spermatid development (25). Recent observations that myotubularin is also expressed in both Sertoli's and germ cells (26) raise the possibility that phosphatases and pseudophosphatases of this family may function on convergent pathways in spermatogenesis. Several lines of evidence strongly suggest that these proteins are likely to impact specific aspects of lipid-mediated signaling. Sbf1 contains a pleckstrin homology (PH) domain that is responsive to phosphatidylinositol 3-kinase in yeast (27) and thus likely to bind phosphatidylinositol lipids. Sbf1 also contains a motif of unknown function shared with Rab3 GEFs (7) involved in vesicular transport or secretory pathways controlled by the Rab family of GTPases (28). Myotubularin itself dephosphorylates phosphatidylinositol 3-phosphate [PI(3)P] (6, 29) and the presence of PI(3)P-binding FYVE domains in other members of this family (15) implies that myotubularin phosphatases regulate signaling by lipid second messengers. Germline mutations of myotubularin are associated with X-linked myotubular myopathy (XLMTM), a congenital disorder characterized by impaired terminal differentiation of myoblasts (4). Several XLMTM mutations consist of single amino acid substitutions in the phosphatase catalytic pocket of myotubularin and abrogate its ability to dephosphorylate PI(3)P (6), implying that phosphatase activity is critical for its function. Furthermore, a phosphatase-defective myotubularin mutant causes an accumulation of PI(3)P in mammalian cells when hyperexpressed (6). Similar inactivating mutations in the myotubularin-related phosphatase MTMr2 are associated with Charcot-Marie Tooth syndrome (7). Since Sbf1 shares extensive sequence similarity with the myotubularin catalytic pocket, these data raise the possibility that myotubularin-related pseudophosphatases may also regulate, or be regulated by, cellular levels of PI(3)P.

Although Sbf1 or other myotubularin-related proteins have not yet been linked to specific signaling pathways, several pathways are known to affect the premeiotic and meiotic progression of pachytene spermatocytes. For instance, the MAP kinase ERK1 is specifically activated during the G2/M transition in spermatocytes (30). Furthermore, mice harboring mutations in the c-*kit* tyrosine kinase receptor display defective spermatogenesis characterized by a block at the premeiotic stage (31). The c-*kit* mutation in these mice disrupts PI 3′-kinase binding and abrogates phosphatidylinositol signaling via Akt (32). Structural features suggest that Sbf1 may function in response to phosphatidylinositol-mediated signaling, however the implicated lipid substrate and *Sbf1*$^{-/-}$ testicular phenotype are different from those associated with c-*kit*. In vitro studies suggest a possible role for Sbf1 in modulating the properties of SET domain proteins such as

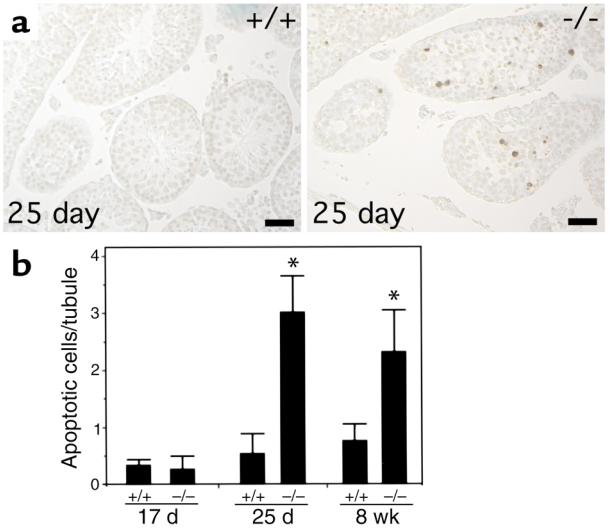


**Figure 7**
Germ cell death in juvenile and adult mouse testis. (**a**) Sections of testis from 25-day-old mice were labeled by TUNEL assay and counterstained with methyl green (×200). Scale bars, 25 μm. (**b**) Quantitation of apoptotic cells per seminiferous tubule based on TUNEL labeling of testis at different stages in mouse testicular development (three mice per time point). *$P$ < 0.05 compared with wild-type.

MLL and Suv39h1 (9, 11). In support of this, a purified protein complex containing *Drosophila* trithorax (homologue of MLL) also contained dSbf1 and dCBP (33). Interestingly, mice that are compound null for Suv39h1 and the related Suv39h2 display chromosomal mis-segregation during meiosis and apoptosis of pachytene spermatocytes (34). Since Sbf1 interacts with and modulates the transcriptional properties of Suv39h1 in vitro (11), and the timing of the testicular defect in *Sbf1*$^{-/-}$ mice also occurs in meiosis, an etiologic relationship of Sbf1 deficiency with Suv39h protein malfunction is possible. However, our own data using spermatocyte gene markers show that pachytene spermatocytes are not initially lost in *Sbf1*$^{-/-}$ mice, suggesting that the Sbf1 and Suv39h testicular defects may result from unrelated mechanisms. Nevertheless, this issue warrants further investigation.

Approximately 40% of cases of human male infertility are idiopathic (35). Gene-knockout studies in mice have identified autosomal genes involved in spermatogenesis, but only three candidate genes (AZFa–AZFc) have been reported in humans. Mutations in the AZF genes are the etiological factors in 10–15% of cases of idiopathic azoospermia and severe oligozoospermia (36, 37). Since these genes account for a small proportion of inherited spermatogenic defects, our studies raise the possibility that Sbf1 deficiency may contribute to human male sterility. Therefore, further studies would appear to be warranted to search for hereditary mutations of Sbf1 in appropriate families.

## Acknowledgments

This work was supported by a grant from the NIH (CA-55029). R. Firestein was supported by a training grant from the National Institute of General Medical Sciences (5T32GM07365). We thank Bich-Tien Rouse for Ab preparation, Eva Pfendt for immunohistochemistry, and Caroline Tudor for photographic assistance.

1. Denu, J.M., Stuckey, J.A., Saper, M.A., and Dixon, J.E. 1996. Form and function in protein dephosphorylation. *Cell.* **87**:361–364.
2. Wishart, M.J., and Dixon, J.E. 1998. Gathering STYX: phosphatase-like form predicts functions for unique protein-interaction domains. *Trends Biochem. Sci.* **23**:301–306.
3. Hunter, T. 1998. Anti-phosphatases take the stage. *Nat. Genet.* **18**:303–305.
4. Laporte, J., et al. 1996. A gene mutated in X-linked myotubular myopathy defines a new putative tyrosine phosphatase family conserved in yeast. *Nat. Genet.* **13**:175–182.
5. Firestein, R., and Cleary, M.L. 2001. Pseudo-phosphatase Sbf1 contains an N-terminal GEF homology domain that modulates its growth regulatory properties. *J. Cell Sci.* **114**:2921–2927.
6. Taylor, G., Maehama, T., and Dixon, J.E. 2000. Myotubularin, a protein tyrosine phosphatase mutated in myotubular myopathy, dephosphorylates the lipid second messenger, phosphatidylinositol 3-phosphate. *Proc. Natl. Acad. Sci. USA.* **97**:8910–8915.
7. Bolino, A., et al. 2000. Charcot-Marie-Tooth type 4B is caused by mutations in the gene encoding myotubularin-related protein-2. *Nat. Genet.* **25**:17–19.
8. Ali, I.U., Schriml, L.M., and Dean, M. 1999. Mutational spectra of PTEN/MMAC1 gene: a tumor suppressor with lipid phosphatase activity. *J. Natl. Cancer Inst.* **91**:1922–1932.
9. Cui, X., et al. 1998. Association of SET domain and myotubularin-related proteins modulates growth control. *Nat. Genet.* **18**:331–337.
10. De Vivo, I., Cui, X., Domen, J., and Cleary, M.L. 1998. Growth stimulation of primary B cell precursors by the anti-phosphatase Sbf1. *Proc. Natl. Acad. Sci. USA.* **95**:9471–9476.
11. Firestein, R., Cui, X., Huie, P., and Cleary, M.L. 2000. Set domain-dependent regulation of transcriptional silencing and growth control by SUV39H1, a mammalian ortholog of *Drosophila* Su(var)3-9. *Mol. Cell. Biol.* **20**:4900–4909.
12. Flint, A.J., Tiganis, T., Barford, D., and Tonks, N.K. 1997. Development of "substrate-trapping" mutants to identify physiological substrates of protein tyrosine phosphatases. *Proc. Natl. Acad. Sci. USA.* **94**:1680–1685.
13. Salanova, M., et al. 1999. Type 4 cyclic adenosine monophosphate-specific phosphodiesterases are expressed in discrete subcellular compartments during rat spermiogenesis. *Endocrinology.* **140**:2297–2306.
14. Print, C.G., et al. 1998. Apoptosis regulator bcl-w is essential for spermatogenesis but appears otherwise redundant. *Proc. Natl. Acad. Sci. USA.* **95**:12424–12431.
15. Laporte, J., et al. 1998. Characterization of the myotubularin dual specificity phosphatase gene family from yeast to human. *Hum. Mol. Genet.* **7**:1703–1712.
16. Yoshida, K., et al. 1998. The mouse RecA-like gene Dmc1 is required for homologous chromosome synapsis during meiosis. *Mol. Cell.* **1**:707–718.
17. Wakayama, T., and Iseki, S. 1999. Specific expression of the mRNA for 25 kDa heat-shock protein in the spermatocytes of mouse seminiferous tubules. *Anat. Embryol. (Berl.)* **199**:419–425.
18. Wu, J.Y., and Means, A.R. 2000. Ca(2+)/calmodulin-dependent protein kinase IV is expressed in spermatids and targeted to chromatin and the nuclear matrix. *J. Biol. Chem.* **275**:7994–7999.
19. Bellve, A.R., et al. 1977. Spermatogenic cells of the prepuberal mouse. Isolation and morphological characterization. *J. Cell. Biol.* **74**:68–85.
20. Gondos, B., and Berndston, W.E. 1993. Sertoli cell toxicants. In *The Sertoli cell*. L.D. Russell and M.D. Griswold, editors. Cache River Press. Clearwater, Florida, USA. 552–575.
21. Chapin, R.E., Morgan, K.T., and Bus, J.S. 1983. The morphogenesis of testicular degeneration induced in rats by orally administered 2,5-hexanedione. *Exp. Mol. Pathol.* **38**:149–169.
22. Boekelheide, K. 1993. Sertoli cell toxicants. In *The Sertoli cell*. L.D. Russell and M.D. Griswold, editors. Cache River Press. Clearwater, Florida, USA. 552–575.
23. Creasy, D.M., Foster, J.R., and Foster, P.M. 1983. The morphological development of di-N-pentyl phthalate induced testicular atrophy in the rat. *J. Pathol.* **139**:309–321.
24. Ogawa, T. 2001. Spermatogonial transplantation: the principle and possible applications. *J. Mol. Med.* **79**:368–374.
25. Wishart, M.J., and Dixon, J.E. 2002. The archetype STYX/dead-phosphatase complexes with a spermatid mRNA-binding protein and is essential for normal sperm production. *Proc. Natl. Acad. Sci. USA.* **99**:2112–2117.
26. Li, J.C., et al. 2000. Rat testicular myotubularin, a protein tyrosine phosphatase expressed by Sertoli and germ cells, is a potential marker for studying cell-cell interactions in the rat testis. *J. Cell Physiol.* **185**:366–385.
27. Isakoff, S.J., et al. 1998. Identification and analysis of PH domain-containing targets of phosphatidylinositol 3-kinase using a novel in vivo assay in yeast. *EMBO J.* **17**:5374–5387.
28. Martinez, O., and Goud, B. 1998. Rab proteins. *Biochim. Biophys. Acta.* **1404**:101–112.
29. Blondeau, F., et al. 2000. Myotubularin, a phosphatase deficient in myotubular myopathy, acts on PI 3-kinase and phosphatidylinositol 3 phosphate pathway. *Hum. Mol. Genet.* **9**:2223–2229.
30. Sette, C., et al. 1999. Activation of the mitogen-activated protein kinase ERK1 during meiotic progression of mouse pachytene spermatocytes. *J. Biol. Chem.* **274**:33571–33579.
31. Kissel, H., et al. 2000. Point mutation in kit receptor tyrosine kinase reveals essential roles for kit signaling in spermatogenesis and oogenesis without affecting other kit responses. *EMBO J.* **19**:1312–1326.
32. Blume-Jensen, P., et al. 2000. Kit/stem cell factor receptor-induced activation of phosphatidylinositol 3′-kinase is essential for male fertility. *Nat. Genet.* **24**:157–162.
33. Petruk, S., et al. 2001. Trithorax and dCBP acting in a complex to maintain expression of a homeotic gene. *Science.* **294**:1331–1334.
34. Peters, A.H., et al. 2001. Loss of the Suv39h histone methyltransferases impairs mammalian heterochromatin and genome stability. *Cell.* **107**:323–337.
35. Kretser, D.M. 1997. Male infertility. *Lancet.* **349**:787–790.
36. Ferlin, A., Moro, E., Garolla, A., and Foresta, C. 1999. Human male infertility and Y chromosome deletions: role of the AZF-candidate genes DAZ, RBM and DFFRY. *Hum. Reprod.* **14**:1710–1716.
37. Hargreave, T.B. 2000. Genetics and male infertility. *Curr. Opin. Obstet. Gynecol.* **12**:207–219.